# Pattern-Stabilized Decorated Polar Liquid-Crystal Fibers

Alexey Eremin,[1,*] Ulrike Kornek,[1] Stephan Stern,[1] Ralf Stannarius,[1] Fumito Araoka,[2] Hideo Takezoe,[2] Hajnalka Nádasi,[3] Wolfgang Weissflog,[3] and Antal Jákli[4]

[1]*Otto-von-Guericke Universität Magdeburg, Institute for Experimental Physics, ANP, 39016 Magdeburg, Germany*
[2]*Department of Organic and Polymeric Materials, Tokyo Institute of Technology, 2-12-1 O-okayama, Meguro-ku, Tokyo 152-8552, Japan*
[3]*Martin Luther University Halle-Wittenberg, Institute of Chemistry, Physical Chemistry, Von-Danckelmann-Platz 4, 06120 Halle, Germany*
[4]*Kent State University, Liquid Crystal Institute, Kent, Ohio 44242, USA*

(Received 14 March 2012; published 6 July 2012)

Geometric frustration gives rise to new fundamental phenomena and is known to yield the formation of exotic states of matter, such as incommensurate crystals, modulated liquid-crystalline phases, and phases stabilized by defects. In this Letter, we present a detailed study of polar structure of freely suspended fluid filaments in a polarization modulated liquid-crystal phase. We show that a periodic pattern of polarization-splay stripes separated by defect boundaries and decorating smectic layers can stabilize the structure of fluid fibers against the Rayleigh-Plateau instability. The instability is suppressed by the resistance of the defect structure to a radial compression of the cylindrical fibers. Our results provide direct experimental observation of a link between the stability of the liquid fibers, internal polar order, and geometrical constraints. They open a new perspective on a wide range of fluid polar fiber materials.

DOI: 10.1103/PhysRevLett.109.017801 PACS numbers: 61.30.−v, 61.30.Jf, 77.84.Nh

The formation of freestanding fluid structures is one of the most striking rheological phenomena observed in non-Newtonian liquids. It can be found not only in scientifically interesting systems such as spider silk or polymeric melts, but also in the processing of industrially important systems such as textile and optical fibers [1–10]. In many cases, the fibers represent solidified liquids or glasses, where the initial stage of fiber formation starts from a liquid. The Rayleigh-Plateau instability [11,12] prevents Newtonian liquids from forming stable liquid filaments. It was shown that structured liquids, such as liquid crystals (LCs), could be more suitable for the formation of stable and very robust fibers [2,4,6–10]. For instance, natural silk is initially spun from a lyotropic nematic liquid. Another example of a liquid-crystalline fiber-forming material is cellulose, which can be electrospun from a cholesteric solution [12–14]. However, experiments with pure thermotropic liquid crystals have shown that the orientational anisotropy of nematics alone does not affect the filament stability [4,6,15]. Even a smectic layer structure in the conventional smectic-*A* (Sm*A*) liquid crystals of rod-shaped molecules can only slightly improve the stability of the LC fibers in air [13,14,16,17]. A single liquid-crystalline system forming freely suspended filaments previously reported was a discotic LC stabilized by its 1D columnar order [4,8,15]. A similar stabilization mechanism can also be realized in the polarization-modulated smectic-*CP* phase (PM-Sm*CP* or $B_7$ phase) [1,16–18].

The PM-Sm*CP* phase shows a wide variety of complex microscopic structures, including labyrinthine patterns in thin films, screwlike and telephone-wire helical filaments in isotropic melt [Fig. 1(a)], and free-standing filaments in air [Fig. 1(b)] [1,8,19]. The PM-Sm*CP* phase is characterized by a chiral structure of the layers due to molecular tilt respective to the layer normal and the spontaneous splay of the molecular bows (designated by the *p* director) which is associated with a spontaneous polarization splay [Figs. 1(c) and 1(d)]. A periodic pattern consisting of stripes of splayed director field separated by grainy boundaries decorates the layers of the PM-Sm*CP* phase. Such a topological constraint leads to a global modulated structure of the director splay stripes, coupled to a layer undulation and separated by defect boundaries. In this study, we explore the role of polarity and modulation in the fiber structure stabilization.

Geometric frustration yields exotic phases in liquid crystals like the twist grain boundary (TGB) phase, dark conglomerate phase, and many others [1,8,18–22]. Geometrically frustrated systems driven by competition between several free-energy contributions favoring different ground states are known to have a degenerate manifold of exotic states with periodic structures [1,19,20,23–25]. As we shall show in this Letter, one-dimensional decoration of smectic layers provides a generic mechanism which is capable of stabilizing smectic LC fibers. In the polarization modulated phase, the stabilization is achieved by an intricate interplay between the polar order, layer chirality, and the coupling between the director deformation and the layer curvature. One example of the polarization modulated phase was found in a bent-core liquid-crystal compound shown in inset of Fig. 1(b). The synthesis and characterization of this compound is described in

 

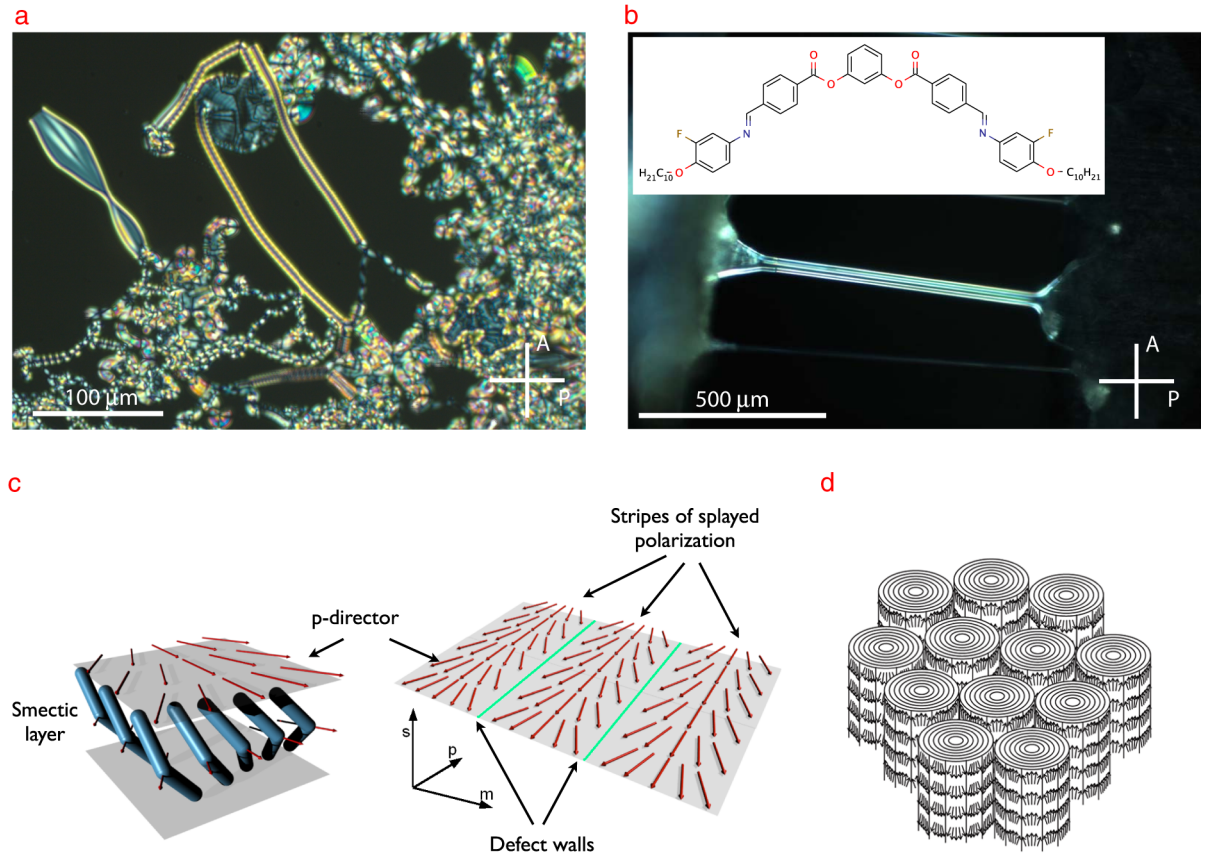


FIG. 1 (color online). Polarizing optical microscope (POM) images and molecular alignment in the PM-Sm$CP$ phase. (a) texture of a 10-$\mu$m-thick cell at the transition from the isotropic phase to the PM-Sm$CP$ phase. (b) POM image of freestanding (in air) filaments in the PM-Sm$CP$ phase ($T = 155\,^{\circ}$C, image width 1.5 mm), the chemical formula of the compound is given in the inset. (c) Schemes of the director configuration (polarization modulated structure) in a single layer of the PM-Sm$CP$ phase. The arrows indicate the direction of the molecular bows ($p$ director). (d) Schematic presentation of a filament bundle structure. The smectic layers form a concentric nested cylinder resulting in a nested-cylinder structure. The optical slow axis is aligned radially, perpendicular to the axis of the fiber.

Refs. [1,26,27]. It shows the following phase sequence: Cr $\overset{129\,^{\circ}\mathrm{C}}{\leftrightarrow}$ ($B_4$ $\overset{98\,^{\circ}\mathrm{C}}{\leftrightarrow}$) Sm$CP_A$ $\overset{136\,^{\circ}\mathrm{C}}{\leftrightarrow}$ PM-Sm$CP$ $\overset{166\,^{\circ}\mathrm{C}}{\leftrightarrow}$ isotropic, where Sm$CP_A$ is a nonmodulated antiferroelectric smectic-$C$ phase (see Refs. [20–22,26] for details) and the PM-Sm$CP$ phase is a polarization modulated layer undulated phase with the undulations described by a rectangular lattice [18]. The freestanding filaments in the PM-Sm$CP$ phase, appear optically as single birefringent fibers (approximately 2 $\mu$m in diameter) or as bundles of fibers with an overall diameter of up to 500 $\mu$m [Figs. 1(b) and 1(d)]. The structure of those filaments has been investigated using x-ray scattering and electron microscopy techniques [20,26,28]. Synchrotron x-ray studies have shown that the smectic layers are modulated also in the fiber geometry [1,26,28]. The direction of the modulation is nearly perpendicular to the axis of the fibers.

To gain insight into the polar properties of the liquid-crystal fibers, we measured optical second-harmonic generation (SHG) in filaments in transmission geometry [Fig. 2(a)]. Experiments on SHG have been performed using a Nd:YAG laser operating at $\omega = 1064$ nm (10 ns pulse width and 10 Hz repetition rate). The SHG signal was detected in transmission geometry by a photomultiplier tube (Hamamatsu). For SHG microscopy, the same laser was employed. The signal acquisition was done using high-sensitive CCD camera (ORCA, Hamamatsu). The fibers show a strong SHG activity. The $s$-$s$ component, i.e., with the electric field parallel to the fiber axis both for fundamental and SHG light, is much stronger than the perpendicular $p$-$p$ component [Fig. 2(b)]. The SHG activity of the filaments indicates that the fibers are polar and the polar axis is aligned parallel to their geometrical axis. In contrast, the bulk samples and thin films show much weaker SHG activity resulting from a global antiferroelectric structure formed by the polarization-splay domains. As the filament is cooled down, the integral SHG signal intensity decreases and disappears upon the transition into the antiferroelectric Sm$CP$ phase. The $s$-$s$ component steeply decreases upon cooling. A slight increase of the $p$-$p$ component can be attributed to a loss of alignment of the polar order due to the

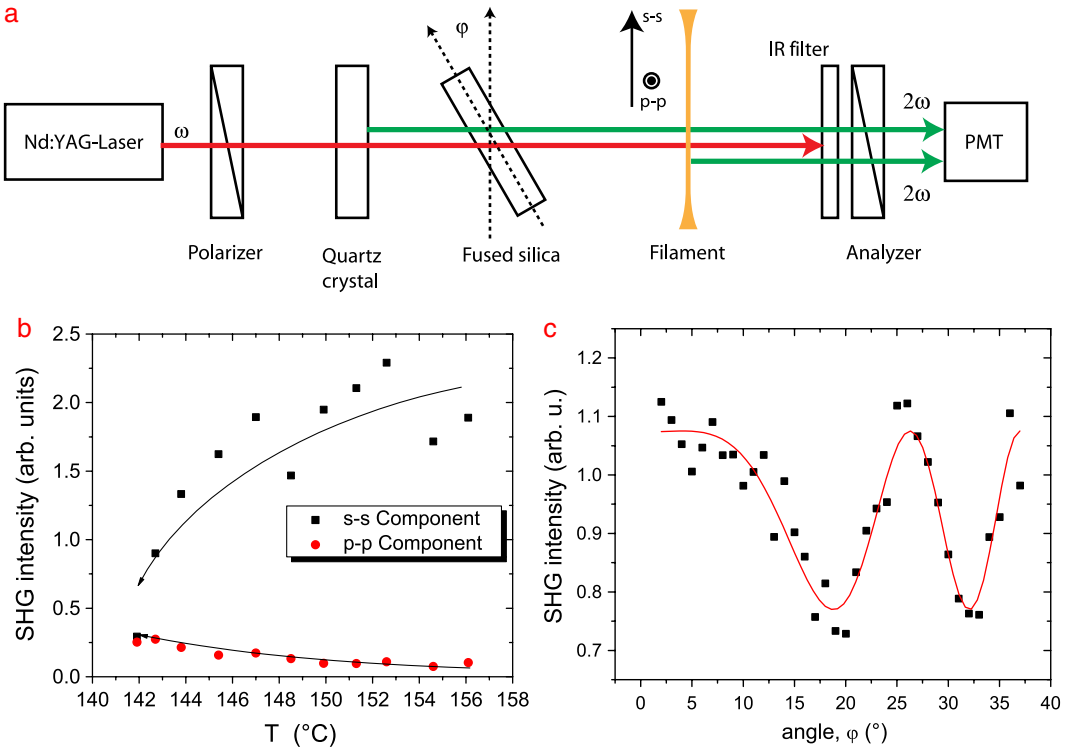


FIG. 2 (color online). SH generation in filaments. (a) Optical setup for SHG interferometry. In this geometry the SHG signal of the filament interferes with that of a quartz crystal constructively or destructively depending on the rotation angle of a thin glass plate, resulting in a fringe structure. (b) Temperature dependence of *p-p* and *s-s* components of SHG intensity (filament thickness 150 $\mu$m). (c) SHG interferogram for SHG signal from a thick filament. Measurements on several other filaments of the same thickness show nearly the same phase, which means that the polar directional sense is the same in every filament.

destabilization of the filaments and an anomalous melting observed on slow cooling into the Sm*CP* phase [1,26].

To investigate the details of the polar structure of the fibers, we performed spatially resolved SHG microscopy studies combined with SHG interferometry. SHG interferometer was built, as shown in Fig. 2(a), using a thin quartz plate as a reference SHG-source. The mutual phase difference between SHG signals from the sample and the quartz plate was varied by rotating a fused silica glass plate. Light- and SHG microscopy images of a filament with

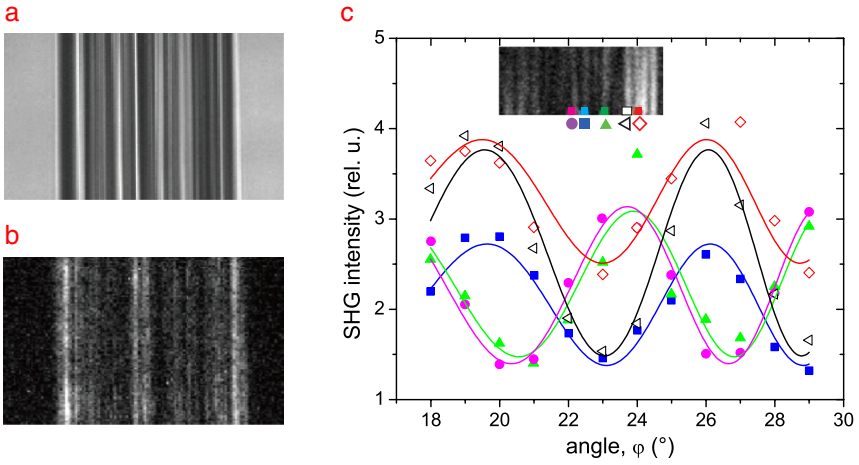


FIG. 3 (color online). SHG-interferometry microscopy. (a) Optical image of the fiber. (b) SHG image of the fiber. The SHG activity of the fibers indicates their polar nature. (c) SHG interferogram for each fiber. SHG microscopy interferometry technique allows us to determine the polar directional sense of each fiber. Opposite polar direction results in a phase shift of $\pi$. In our case one can differentiate between the fibers polarized in parallel or antiparallel directions with respect to the pulling direction.

radius 95 $\mu$m are shown in Figs. 3(a) and 3(b), respectively. The SHG image reveals a filament consisting of fine bright stripes corresponding to single fibers. The fiber diameter is about 2 $\mu$m which is in good agreement with the value obtained using scanning electron and atomic force microscopy techniques [26,28–30]. The SHG signals from fibers aligned with antiparallel polar senses are in antiphase, so they interfere destructively. In contrast, the signals from fibers with the same polar sense interfere constructively. This explains the presence of darker and brighter stripes in the SHG image. To further determine the directional sense of the nonlinear polarization, we performed SHG-interferometry measurements [Fig. 2(a)]. The SHG signal intensity from the filament (bundle of fibers) displays interference fringes [Fig. 2(c)]. In order to investigate the mutual polar order within each fiber, the SHG interferogram was measured from single fibers in a filament bundle. The result is shown in Fig. 3(c). The data are categorized into two groups, which have a mutual phase shift of $\pi$, indicating the existence of fibers with parallel and antiparallel polar orders along the fiber axis. The similar amplitudes of the SHG interferograms for all the fibers suggest that the polar directional sense is unique within each fiber. Almost uniform brightness of SHG images along each fiber supports this conclusion. One possible origin of this symmetry breaking may originate from the fact that the mesogens become flow aligned during the pulling process. It is the first example of fluid, but stable, polar fibers.

One could imagine a stable fiber formation in media with hardly compressible layers, since the radius fluctuations of fibers would be prohibited and only the rupture of layers can lead to a modulation of the radius. In fact, filament formation is not possible in conventional smectic liquid crystals, such as Sm*A* and Sm*C*, in air. Similar to ordinary liquids, smectic liquid-crystal cylinders are susceptible to the Rayleigh-Plateau instability, which occurs when the length of a cylinder is slightly larger than $\pi$ times the diameter [4,15,28–30]. The instability of smectic cylinders may originate from the fact that a redistribution of the material in the isotropic core radius requires no layer compression. This can be achieved by axial flow of the bulk material, in particular, into and out of the meniscus where the filament is attached [Figs. 4(a) and 4(b)]. It is important to note that the filaments are stable in the SHG-active PM-Sm*CP* phase and become unstable upon cooling into the nonmodulated antiferroelectric Sm*CP* state [4,15,26], where SHG activity is lost, although the difference between the two phases is marginal.

A possible explanation for the stability of the filaments has been proposed by Bailey *et al.* It assumes local triclinic symmetry of the phase structure with out-of-plane polarization (Sm$C_G$ phase) [26,29,31]. An additional component of the spontaneous polarization enhances the effective compression modulus, suppressing the Rayleigh-Plateau

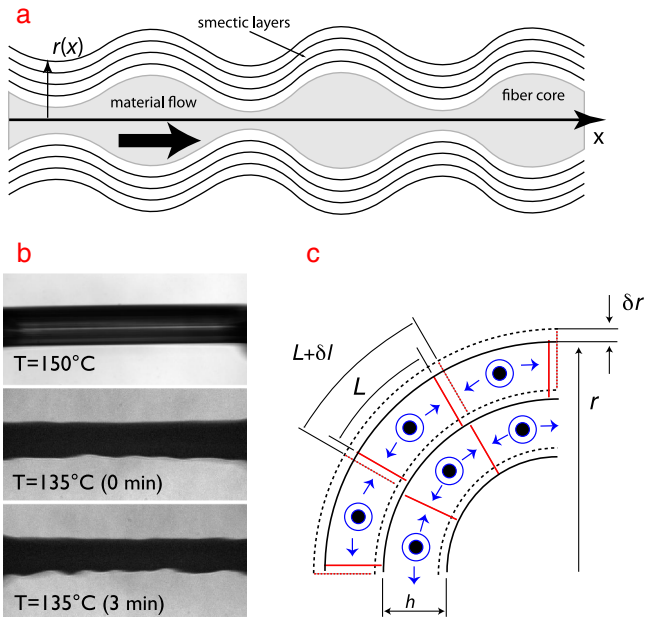


FIG. 4 (color online). Unstable and stable fibers made of concentric smectic layers. (a) A scheme of an unstable fiber without layer decoration. Any change of the radius is allowed with a help of materials flow from the meniscus. (b) Optical microscopy images of unstable filaments (dark images) upon the transition into the nonmodulated Sm*CP* phase (image width 600 $\mu$m). (c) Polarization-splay stripes in two subsequent smectic layers in a fiber. A slight increase of the curvature radius $\delta r$ results in a deviation of the stripe width $\delta l$ from its equilibrium value.

instability. Local triclinic symmetry can also lead to modulation in the direction perpendicular to the layer normal [29,31]. Here we propose an alternative mechanism of fiber stabilization, which is based on the simple layer decoration with a periodic pattern due to the polarization-splay (PS) modulation. The PS modulation [Fig. 1(c)] is characterized by a length scale corresponding to the width of the PS stripes. Small modulations of the radius of a filament would require the deviation of the stripe width from its equilibrium value [Fig. 4(c)]. Such a change results in an increase of the elastic energy stored in the fiber. The energy change can be estimated using a linear div **P** term in the free-energy density responsible for the periodic modulation structure of the liquid-crystal phase [1,31]. Assuming a periodic radius modulation $R(x) = R_0 + \delta r \cos(qx)$ along the filament axis with a wave number $q$ [Fig. 4(a)], the free-energy gain is determined by the filament radius $R_0$ and surface tension $\sigma$, and given by (see Supplemental Material [32] for derivation)

$$\Delta F = \frac{\pi\sigma\delta r^2}{2R_0}\left(R_0{}^2q^2 + \frac{aR_0}{\pi\sigma} - 1\right),$$

where the contribution of the polarization-splay pattern with spontaneous splay $s_0$ is given by an effective

compression modulus $a = \pi K s_0^2 \ln(R_0/r_c)$ ($r_c$ is the radius of the fiber core). This equation shows that the Rayleigh-Plateau instability can be completely suppressed if the compression term exceeds 1. The critical radius can be estimated if one assumes typical values for the elastic constant $K \sim 10^{-11}$ N, core radius $r_c \sim 10^{-8}$ m [33], spontaneous splay $s_0 \sim 10^7$ m$^{-1}$ [1,18], one obtains a critical radius of 4 $\mu$m which is in the same order of magnitude as experimentally observed fibers. The effective compression modulus $a$ is in the range of 10–20 kPa. This model explains the absolute stability of the fibers with radii above the critical value.

In summary, we have presented clear experimental evidence of spontaneous polar order in liquid-crystalline filaments formed in PM-Sm*CP*. By spatially resolved SHG-interferometry technique, we prove that the filaments are composed of nearly monodisperse polar fibers. The stability of the fibers is sustained by a periodic pattern of polarization-splay stripes separated by defect boundaries decorating the smectic layers with liquidlike in-plane order. This type of stabilization is a result of a geometrical incompatibility of the polarization-splay deformation and the geometry of a layer plane, which yields a new length scale defined by a balance between the elastic energy and the energy of the defect nucleation. This stabilization mechanism is generic and can be found in wide range of systems resulting in a manifold of different morphologies. Finally, we believe that such materials offer significant potential to advance our understanding of the role of geometrical frustration in the formation and stability of structures formed by complex anisotropic fluids.

The research was supported by Deutsche Forschungsgemeinschaft (ER 467/2-2). The support of Tokyo Tech G-COE Program is appreciated. The authors thank H. Sawade (TU Berlin) for supplying sample materials.

*alexey.eremin@ovgu.de

[1] D. A. Coleman, J. Fernsler, N. Chattham, M. Nakata, Y. Takanishi, E. Korblova, D. R. Link, R.-F. Shao, W. G. Jang, J. E. Maclennan, O. Mondainn-Monval, C. Boyer, W. Weissflog, G. Pelzl, L.-C. Chien, J. Zasadzinski, J. Watanabe, D. M. Walba, H. Takezoe, and N. A. Clark, Science **301**, 1204 (2003).

[2] J. Fontana, C. Bailey, W. Weissflog, I. Jánossy, and A. Jákli, Phys. Rev. E **80**, 032701 (2009).

[3] L. Hough, M. Spannuth, M. Nakata, and D. Coleman, Science **325**, 452 (2009).

[4] A. G. Cheong, A. D. Rey, and P. T. Mather, Phys. Rev. E **64**, 041701 (2001).

[5] B. A. DiDonna and R. D. Kamien, Phys. Rev. Lett. **89**, 215504 (2002).

[6] F. Vollrath and D. Knight, Nature (London) **410**, 541 (2001).

[7] K. Kerkam, C. Viney, D. Kaplan, and S. Lombardi, Nature (London) **349**, 596 (1991).

[8] D. H. Van Winkle and N. A. Clark, Phys. Rev. Lett. **48**, 1407 (1982).

[9] T. R. Wolinski, S. Ertman, P. Lesiak, A. W. Domanski, A. Czapla, R. Dabrowski, E. Nowinowski-Kruszelnicki, and J. Wojcik, Opto-Electron. Rev., **14**, 329 (2006).

[10] E. Ozbay, Science **311**, 189 (2006).

[11] C. Patrick Royall, S. R. Williams, T. Ohtsuka, and H. Tanaka, Nature Mater. **7**, 556 (2008).

[12] S. Chandrasekhar, *Hydrodynamic and Hydromagnetic Stability* (Dover Publications, New York, 1961).

[13] M. H. Godinho, J. P. Canejo, G. Feio, and E. M. Terentjev, Soft Matter **6**, 5965 (2010).

[14] P. L. Almeida, S. Kundu, J. P. Borges, M. H. Godinho, and J. L. Figueirinhas, Appl. Phys. Lett. **95**, 043501 (2009).

[15] M. Mahajan, M. Tsige, P. Taylor, and C. Rosenblatt, Liq. Cryst. **26**, 443 (1999).

[16] M. Todorokihara, Y. Iwata, and H. Naito, Phys. Rev. E **70**, 021701 (2004).

[17] A. Jákli, C. Lischka, W. Weissflog, G. Pelzl, and A. Saupe, Liq. Cryst. **27**, 1405 (2000).

[18] D. A. Coleman, C. D. Jones, M. Nakata, N. A. Clark, D. M. Walba, W. Weissflog, K. Fodor-Csorba, J. Watanabe, V. Novotna, and V. Hamplova, Phys. Rev. E **77**, 021703 (2008).

[19] A. Jákli, D. Krüerke, and G. G. Nair, Phys. Rev. E **67**, 051702 (2003).

[20] R. D. Kamien and J. V. Selinger, Condens. Matter Phys. **13**, R1 (2001).

[21] R. D. Kamien and T. C. Lubensky, Phys. Rev. Lett. **82**, 2892 (1999).

[22] K. J. Ihn, J. A. Zasadzinski, R. Pindak, A. J. Slaney, and J. Goodby, Science **258**, 275 (1992).

[23] N. Ikeda, H. Ohsumi, and H. Kitô, Nature (London) **436**, 1136 (2005).

[24] M. Angst, R. P. Hermann, W. Schweika, J.-W. Kim, P. Khalifah, H. J. Xiang, M.-H. Whangbo, D.-H. Kim, B. C. Sales, and D. Mandrus, Phys. Rev. Lett. **99**, 256402 (2007).

[25] Y. Han, Y. Shokef, A. M. Alsayed, P. Yunker, T. C. Lubensky, and A. G. Yodh, Nature (London) **456**, 898 (2008).

[26] A. Eremin, A. Nemes, R. Stannarius, M. Schultz, H. Nádasi, and W. Weissflog, Phys. Rev. E **71**, 031705 (2005).

[27] H. Nádasi, Ph.D. thesis, Martin-Luther-Universität Halle, Halle (Saale), 2004.

[28] A. Nemes, A. Eremin, R. Stannarius, M. Schulz, H. Nádasi, and W. Weissflog, Phys. Chem. Chem. Phys. **8**, 469 (2006).

[29] C. Bailey, E. C. Gartland, and A. Jákli, Phys. Rev. E **75**, 031701 (2007).

[30] C. Bailey, M. Murphy, A. Eremin, W. Weissflog, and A. Jakli, Phys. Rev. E **81**, 031708 (2010).

[31] C. Bailey and A. Jákli, Phys. Rev. Lett. **99**, 207801 (2007).

[32] See Supplemental Material at http://link.aps.org/supplemental/10.1103/PhysRevLett.109.017801 for the derivation of the formula for the free energy of the fiber.

[33] P. G. de Gennes and J. Prost, *The Physics of Liquid Crystals* (Clarendon Press, Oxford, 1993).